Sensors and Actuators B 251 (2017) 763–772

Contents lists available at ScienceDirect

Sensors and Actuators B: Chemical

journal homepage: www.elsevier.com/locate/snb

Research paper

Molecularly imprinted surface plasmon resonance (SPR) sensor for uric acid determination

Aslı Göçenoğlu Sarıkaya[a], Bilgen Osman[a,*], Tülay Çam[a], Adil Denizli[b]

[a] Department of Chemistry, Uludağ University, Bursa, Turkey
[b] Department of Chemistry, Hacettepe University, Ankara, Turkey

ARTICLE INFO

Article history:
Received 2 November 2016
Received in revised form 10 May 2017
Accepted 16 May 2017
Available online 20 May 2017

Keywords:
Uric acid
SPR sensor
Molecular imprinting
Nanoparticle
Metal ion imprinting

ABSTRACT

The main objective of this study was to prepare a surface plasmon resonance (SPR) sensor for uric acid (UA) detection by using molecularly imprinted nanoparticles as a molecular recognition element. For imprinting, metal ion mediated preorganization was performed to interact between template molecules (UA) and functional monomer by using Fe^{3+} ions. UA-imprinted poly (hydroxyethyl methacrylate methacryloyl-L-cysteine methyl ester)-Fe^{3+} [poly(HEMA-MAC)-Fe^{3+}] nanoparticles were synthesized by emulsion polymerization in the presence of MAC-Fe^{3+}-UA pre-polymerization complex. The characterization of UA-imprinted poly(HEMA-MAC)-Fe^{3+} nanoparticles was conducted by Fourier transform infrared spectroscopy (FTIR), elemental analysis, scanning electron microscopy (SEM), energy dispersive x-ray spectroscopy (EDS), transmission electron microscopy (TEM) and zeta size analysis. The SPR sensor was prepared by gold surface modification of the sensor with UA-imprinted poly(HEMA-MAC)-Fe^{3+} nanoparticles. Characterization of the SPR sensor surface was performed with atomic force microscopy (AFM), contact angle (CA) and optic profilometer measurements. UA sensing ability of the prepared sensor was determined by interacting UA solutions in different concentrations (0.5–40 mg/L) with the SPR sensor. The limit of detection (LOD) and limit of quantification (LOQ) values for the prepared SPR sensor were calculated as 0.247 and 0.825 mg/L for aqueous solution, respectively. The UA-imprinted sensor was also used for UA detection in urine. The results showed the SPR sensor has high selectivity and sensitivity for UA.

© 2017 Elsevier B.V. All rights reserved.

1. Introduction

Uric acid (UA, urate, 2,6,8-trihydroxypurine) is the end product of purine metabolism in the human body [1]. UA is found in biological fluids, such as urine, saliva, blood serum and plasma [2]. UA concentration varies between 100 and 400 μM in the plasma and serum [3]. The concentration in the urine is 250–750 mg/L for adults [4]. Because it may be associated with several diseases – such as hyperuricemia and hypouricemia – the determination of UA in biological samples, especially in serum and urine, is clinically important. Hyperuricemia is caused by increased production of UA or by decreased renal excretion of UA. Hyperuricemia leads to diseases like primary gout, Lesch-Nyhan syndrome and glucose-6-phosphate deficiency and, thus, hyperuricosuria [5,6]. Hypouricemia can result from either a decay of protein synthesis or a defect in renal tubular UA re-adsorption. Abnormal UA concentrations are also linked to hypertension, pneumonia and cardiovascular diseases [7]. Recently, studies have demonstrated that the low UA level in the serum and/or cerebrospinal fluid is a biomarker of Parkinson's disease [8].

Traditional methods used to determine UA in clinical analysis are based on the enzymatic conversion of urate to allantoin or generating CO_2 and H_2O_2 by the use of an uricase enzyme combined with a colorimetric measurement [7], or direct monitoring by ultraviolet spectrophotometry [9]. An alternative method is based on the reduction of phosphotungstic acid to tungsten blue by UA [10]. However, these methods require expensive and labile reagents and also require complex sample preparation steps for the removal of other absorbing components, such as dopamine and ascorbic acid in biological fluids [11]. The most important problem in the vast majority of the chromatographic methods used to detect UA is the need for the deproteinization of serum samples prior to analysis, which involves multiple reaction steps, various sample preparation steps, low detection limit and expensive equipment; can be hindered by low sample throughput, operational

* Corresponding author at: Uludag University, Gorukle Campus, Nilufer, 16059 Bursa, Turkey.
E-mail address: bilgeno@uludag.edu.tr (B. Osman).

http://dx.doi.org/10.1016/j.snb.2017.05.079
0925-4005/© 2017 Elsevier B.V. All rights reserved.

costs and high acquisition; and can generate toxic waste on the side [12,13]. The methods using biosensors have been developed to detect UA due to the advantages of simple measurement, high selectivity, high sensitivity, a short response time, rapid and simple assay procedure, small volume and ease of miniaturization [14]. Most UA biosensors are amperometric, potentiometric [15], chemiluminescence [16], and electrochemical [14] with enzymatic or non-enzymatic methods. On the direct amperometric enzyme sensors, the decrease in dissolved oxygen level is measured by the uricase-catalysed oxidation of UA aside from determination of the amount of the enzymatically generated H_2O_2. However, AA, epinephrine and DA are also electroactive species and generally prevent the correct determination of UA [14]. In addition, the oxidation potential of H_2O_2 is relatively high, and the oxidation potential of AA is very close to that of UA [17]. To solve these problems, many researchers have developed new techniques, such as polymer-modified electrodes [18]. Poly(4-vinylpyridine) [19], polypyrrole [20], poly(*N*,*N*′-dimethylaniline) [21], polyglycine [22], osmium complex Nafion bilayer [23], clay-Nafion [24], methylene blue/sol-gel [25] and self-assembled monolayers of thiols [26], electrochemically pre-treated carbon paste electrodes [27] or clay-modified electrodes [28] were used for modification. However, these techniques are expensive, fragile and time-consuming [29].

In recent years, to improve UA detection with biosensors, molecularly imprinting techniques have been used to develop new approaches [29]. Molecular imprinting is a technique that enables the preparation of synthetic receptors or biomimetic polymeric recognition sites. It attracts rapidly increasing interest as an analytical tool to prepare artificial recognition elements with low cost and high durability. To prepare molecularly imprinted polymer (MIP), functional monomer and cross-linker, which are interacted with a template molecule via non-covalent interactions or reversible covalent bonds, they are polymerized. The removal of the template molecule constitutes specific cavities for the template molecule in the polymer. The prepared polymeric material containing specific binding sites for template molecule (analyte) is an ideal candidate for sensor preparation. The template molecule can be detected by using different physicochemical properties, such as absorbance, fluorescence, luminescence and induced scintillation or surface plasmon resonance (SPR). Molecularly imprinted polymers can be used as recognition elements for the preparation of SPR sensors. SPR-based sensors enable the use of appropriate recognition elements and the determination of chemical and biological compounds without any labelling in real time. However, only limited work has been published using the SPR technique for UA detection. Poly(2–aminobenzylamine)/single wall carbon nanotube thin films were used for UA recognition elements in electrochemical surface plasmon resonance spectroscopy (EC–SPR) technique [30]. The SPR features of the Ag@GO nanocomposite were used for the simultaneous detection of dopamine, ascorbic acid and UA [31]. A simple colorimetric estimation of UA using polyvinyl pyrrolidone-capped-silver nanoparticles was described by Misraa et al. [32]. Though MIP-based sensors have been prepared for UA detection [33–41], to the best of my knowledge, an MIP-based SPR sensor was not reported until now.

In this study, a SPR sensor for UA detection was prepared using molecularly imprinted nanoparticles. A metal ion mediated preorganization step was used for UA molecular imprinting. An Fe^{3+} ion was selected as a metal ion. UA (template molecule) and MAC (methacryloyl-L-cysteine methyl ester, functional monomer) were ligand molecules. The mol ratio of UA/Fe^{3+}/MAC in the MAC-Fe^{3+}-UA pre-polymerization complex was investigated by using a potentiometric titration method. Then, UA-imprinted poly(hydroxyethyl methacrylate methacryloyl-L-cysteine methyl ester)-Fe^{3+} [poly(HEMA-MAC)-Fe^{3+}] nanoparticles were synthesized by using the prepared MAC-Fe^{3+}-UA pre-polymerization complex. HEMA and ethylene glycol dimethacrylate (EGDMA) were comonomer and cross-linker, respectively. The poly(HEMA-MAC)-Fe^{3+} nanoparticles were characterized by Fourier transform infrared spectroscopy (FTIR), elemental analysis, scanning electron microscopy (SEM), energy dispersive x-ray spectroscopy (EDS), transmission electron microscopy (TEM) and zeta size analysis. A UA-imprinted SPR sensor was obtained by dropping and drying a small amount of poly(HEMA-MAC)-Fe^{3+} nanoparticle solution to the SPR sensor gold surface. Then, the SPR sensor surface was characterized by atomic force microscopy (AFM), contact angle (CA) and optical profilometer measurements. The UA detection from aqueous UA solutions was studied. To show selectivity of the UA-imprinted poly(HEMA-MAC)-Fe^{3+} SPR sensor, ascorbic acid (AA), theophylline (Teo) and urea (U) were used as competitor biological molecules. The kinetic and isothermal parameters were elucidated for UA binding. The UA detection capability of the UA-imprinted SPR sensor was also investigated in urine.

2. Experimental

2.1. Materials

HEMA and EGDMA were purchased from Fluka. After the distillation in the presence of hydroquinone inhibitor, they are stored at 4 °C until use. Poly(vinyl alcohol) (PVA; MW: 100,000, 98% hydrolysed) was supplied from Aldrich Chem. Co. (USA). L-cysteine methyl ester hydrochloride, methacryloyl chloride and ammonium persulfate (APS) were purchased from Sigma (St. Louis, USA). All other chemicals were of an analytical grade. The proper amount of $Fe(NO_3)_3{\cdot}9H_2O$ was dissolved to prepare a stock solution of Fe^{3+}. HNO_3 was used to prevent hydrolysis before potentiometric titration. The standardization of the Fe^{3+} stock solution was conducted with complexometric titration by ethylenediaminetetraacetic acid (EDTA) titration using the Schwarzenbach's method [42]. The gold surfaces specific for the SPRimager II were obtained from GWC Technologies (Madison, ABD). Ultra-pure water was obtained by using Elga Flex3 (Veloia Water Solutions & Technologies, France).

2.2. Synthesis of N-methacryloyl-L-cysteine methyl ester monomer

The preparation and characterization of the *N*-methacryloyl-L-cysteine methyl ester (MAC) monomer was given in detail before [43]. Briefly, the following experimental procedure was applied: L-cysteine methyl ester (5.0 g) and hydroquinone (0.2 g) were dissolved in dichloromethane (100 mL). The solution was then cooled to 0 °C and 12.7 g of triethylamine was added. In addition, 5.0 mL of methacryloyl chloride was slowly added to the mixture, followed by stirring at room temperature for 2 h. After the reaction completion, the unreacted components were removed by using 10% NaOH solution. The aqueous phase was evaporated in an evaporator and the monomer (MAC) was crystallized in ethanol and ethyl acetate.

2.3. Potentiometric titrations

Schott Titroline Alpha Plus automatic titrator was used to perform potentiometric titrations. The titrations were carried out in a double-glazed glass cell at a constant temperature (25.0 ± 0.1 °C). A circulating water bath (VWR, precision ±0.1 °C) connected to the glass cell was used to keep the temperature constant. The pH-meter (Mettler-Toledo) was calibrated daily. The calibration of the combined glass electrode was carried out daily from the titration of 0.1 M HCl and 0.1 M NaOH at the same ionic strength before each titration. Additionally, 0.1 M KNO_3 was used to adjust ionic strength of the solutions. The total volume used for each titration was 50 mL.

The methods used in potentiometric titrations can be summarized as follows. Total solution volume for each preparation given below was 50 mL. The solutions prepared in each step were titrated with adjusted KOH solution in the range of pH 2.00–11.00. The titration curves were used for the determination of MAC-Fe^{3+}-, UA-Fe^{3+} and MAC-Fe^{3+}-UA complex stoichiometries.

a. Cell calibration – 5 mL 0.1 M HCl + 5 mL 1 M KNO_3.

b. Determination of inflection points – 5 mL 0.1 M HCl + n mmol ligand (MAC or UA) + 1 M KNO_3 (n = 1–6).

c. Determination of MAC-Fe^{3+} and UA-Fe^{3+} complex stoichiometries – 5 mL 0.1 M HCl + n mmol ligand (MAC or UA) + a mL 0.01 M Fe^{3+} + 5 mL 1 M KNO_3 (n = 1–6).

d. Determination of MAC-Fe^{3+}-UA pre-polymerization complex stoichiometry – 5 mL 0.1 M HCl + n mmol UA + m mmol MAC + a mL 0.01 M Fe^{3+} + 5 mL 1 M KNO_3.

2.4. Preparation of the pre-polymerization complex (MAC –Fe^{3+}-UA)

First, the MAC-Fe^{3+} complex was prepared by adding MAC monomer (0.1 mmol) into $Fe(NO_3)_3{\cdot}9H_2O$ solution (containing 0.05 mmol Fe^{3+} ions) at a stirring rate of 260 rpm for 3 h. Then, the template molecule (UA, 0.1 mmol) was added to the complex molecule mixture rapidly and stirred (260 rpm) for 3 h. After the filtration, the MAC-Fe^{3+}-UA complex was washed with ethanol, followed by drying in a vacuum oven at 50 °C for 24 h. The prepared pre-polymerization complex (MAC-Fe^{3+}-UA) was used for UA-imprinted poly(HEMA-MAC)-Fe^{3+} nanoparticle synthesis.

2.5. Preparation and characterization of the poly(HEMA-MAC)-Fe^{3+}nanoparticles

The emulsion polymerization method was used to prepare UA-imprinted poly(HEMA-MAC)-Fe^{3+} nanoparticles. The UA-imprinted poly(HEMA-MAC)-Fe^{3+} nanoparticles were synthesized by using the following experimental procedure: For the first aqueous phase, 93.8 mg of PVA, 14.43 mg sodium dodecyl sulphate (SDS) and 11.73 mg $NaHCO_3$ were dissolved in 5 mL of deionized water. The second aqueous phase was prepared by dissolving 50 mg PVA and 50 mg SDS in 100 mL of deionized water. The two aqueous phases were then mixed. Then, 12.55 μL of HEMA, 172.45 μL of EGDMA and MAC-Fe^{3+}-UA pre-polymerization complex were added into aqueous solution mixture and slowly agitated for 30 s before being added to the polymerization reactor. Next, 63 mg of ammonium peroxodisulphate (APS) and 57.5 mg $NaHSO_3$ were added in a reactor and polymerized at 40 °C (300 rpm) for 12 h. At the end of the polymerization, the reactor content was cooled to room temperature. To remove unreacted monomers, the UA-imprinted poly(HEMA-MAC)-Fe^{3+} nanoparticles were incubated in ethanol solution (50%) for 1 h. Then, UA-imprinted poly(HEMA-MAC)-Fe^{3+} nanoparticles were further washed with deionized water. The non-imprinted poly(HEMA-MAC)-Fe^{3+} nanoparticles were prepared using the same procedure without adding UA (only MAC-Fe^{3+} complex monomer was used).

The template (UA) was removed from the cleaned nanoparticles using a solution at pH 4.0.The pH of the solution was adjusted using portions of 0.1 M HCl and 0.1 M NaOH. The imprinted nanoparticles were added into the solution at pH 4.0 for 24 h at room temperature, and the procedure was repeated until the template molecule could not be detected in the supernatant with a UV–vis spectrophotometer at 286 nm wavelength.

The morphology of poly(HEMA-MAC)-Fe^{3+} nanoparticles was investigated by using scanning electron microscope (SEM) with an energy dispersive spectroscopy (EDS or EDX) attachment (Jeol, JEM 1200EX, Tokyo, Japan).

UA-imprinted poly(HEMA-MAC)-Fe^{3+} nanoparticles were also visualized by using transmission electron microscope (TEM; JEOL JEM 2100F, USA). The morphology of the nanoparticles was monitored by scanning the sample at the desired magnifications.

Elemental analyses of poly(HEMA-MAC)-Fe^{3+} nanoparticles were carried out by using a LECO elemental analyser (Model CHNS-932, St. Joseph, MI).

An FTIR spectrometer was used to study chemistry of MAC (functional monomer), MAC-Fe^{3+} (complex monomer), MAC-Fe^{3+}-UA (pre-polymerization complex) and UA-imprinted poly(HEMA-MAC)-Fe^{3+}nanoparticles in the solid state (Perkin Elmer, Spectrum 100, USA).

The size distribution of the nanoparticles was investigated by using a Zetasizer Nano-Zeta potential analyser (Malvern Instrument Company, UK).

2.6. Preparation and characterization of the UA-imprinted SPR sensor

First, the gold surface was cleaned by immersing the SPR sensor in an alkaline piranha solution (20 mL, 3:1, NH_4OH:H_2O_2, v/v) for 30 s. After that, the surface was washed several times with ethanol and dried in a vacuum oven (200 mmHg, 40 °C) for 3 h. The cleaned gold surface was modified with allyl mercaptan to increase surface hydrophilicity for coating the nanoparticles onto the surface. For this purpose, the SPR sensor was immersed in a 3.0 mM allyl mercaptan solution prepared in ethanol:water mixture (4:1, v/v) for 12 h. Finally, the gold surface was washed with excess amounts of ethanol and then dried with nitrogen gas under a vacuum (200 mm Hg, 40 °C). The poly(HEMA-MAC)-Fe^{3+} nanoparticles were coated on the modified SPR gold surface by dropping an aliquot (100 μL) of the poly(HEMA-MAC)-Fe^{3+} nanoparticles dispersion onto the gold surface. After the coated surface was dried in vacuum oven (40 °C, 12 h), the UA-imprinted SPR sensor surface was washed with water and ethanol, followed by being dried with nitrogen gas under vacuum (200 mmHg, 40 °C). The preparation procedure for the UA-imprinted nanosensor is depicted in Fig SI1.

The SPR sensor surface was characterized by using an atomic force microscope (AFM; Nanomagnetics Instruments, Oxford, England) in tapping mode. The sample area, scanning rate and resolution were $1 \times 1\ \mu m^2$, 0.7 μm/s and 256 × 256 pixels, respectively. Visualization studies were carried out in non-contact mode.

An Attention KSV instrument (Finland) was used to determine the contact angles of the gold surface, the allyl mercaptan modified gold surface and the UA-imprinted poly(HEMA-MAC)-Fe^{3+} SPR gold surfaces. Five different parts selected in the surfaces and 40 separate photos were taken to measure the contact angles. To calculate the surface free energy (SFE) of the studied surfaces, the contact angles with water, ethylene glycole, diiodomethane and formamide were used by applying the acid–base method.

The coating thickness measurements and 3D visualization studies of the UA-imprinted poly(HEMA-MAC)-Fe^{3+}SPR gold surface were conducted by using an optical profilometer (Zeta Instruments, USA).

2.7. Kinetic, isotherm and selectivity studies with SPR sensor

Kinetic analyses were performed in the SPRImager II system with SPR sensors prepared by coating the UA-imprinted and non-imprinted poly(HEMA-MAC)-Fe^{3+} nanoparticles with allyl mercaptan modified gold surface. In a routine analysis, the sensor surface was washed with a solution at pH 8.0 for 40 min. Then, the resonance angle was set, and the sample solution (aqueous UA solutions or urine samples) was sent to the surface at a flow rate of 150 μL/min after the surface was interacted with the pH 8.0

solution for 2 min more. The SPR sensorgrams were prepared by instantly recording ΔR% values. It was observed that a plateau was reached in about 15 min. A pH 8.0 solution was again sent to the surface to desorb non-specifically bound UA. The regeneration of the surface was carried out using a solution at pH 4.0. At the end of the kinetic analysis, the surface was washed with deionized water and the solution at pH 8.0, respectively.

The concentration dependency of the prepared UA-imprinted SPR sensor was investigated by using UA solutions in the concentration range of 0.5 mg/L–40 mg/L (pH 8.0).

The kinetic and equilibrium isotherm parameters were calculated using equilibrium kinetic analysis and Langmuir, Freundlich and Langmuir–Freundlich (Sips) isotherm models [44]. The linear forms of the models are given as:

$$\textit{Equilibrium Kinetic Analysis} \quad d\Delta R/dt = k_a C\Delta R_{max} - (k_a C + k_d)\Delta R \quad (1)$$

$$\textit{Langmuir} \quad \Delta R = \{\Delta R_{max}[C]/K_D + [C]\} \quad (2)$$

$$\textit{Freundlich} \quad \Delta R = \Delta R_{max}[C]^{1/n} \quad (3)$$

$$\textit{Langmuir} - \textit{Freundlich} \quad \Delta R = \{\Delta R_{max}[C]^{1/n}/K_D + [C]^{1/n} \quad (4)$$

ΔR is the response measured with binding; C is UA concentration (mg/L); 1/n is Freundlich exponent; k_a (mg/L s) and k_d (1/s) are forward and reverse kinetic rate constants; K_A (mg/L) and K_D (L/mg) are forward and reverse equilibrium constants; and the subscript $_{max}$ indicates maximum.

Ascorbic acid (AA), theophylline (Teo), and urea (U) were used as competitor molecules to determine selectivity. Solutions of the competitor molecules in concentrations of 10 mg/L (except urea in the concentration of 100 mg/L) (pH 8.0) were applied to both UA-imprinted (MIP) and non-imprinted (NIP) SPR sensors. The responses of the sensors were determined as ΔR%. In addition, binary, triple and quadruple mixtures of the competing molecules were prepared and interacted with UA-imprinted (MIP) and non-imprinted (NIP) SPR sensors to obtain ΔR% values. The concentration of each competing molecule in the mixtures was 10 mg/L.

The distribution coefficient is used to investigate the binding specificity of the imprinted polymers.

$$K_d = [(C_i - C_f)/C_f] \times V/m \quad (6)$$

Kd (L/mg) is the distribution coefficient, C_i (mg/L) is the concentration of UA solution before binding, C_f (mg/L) is the concentration of the UA solution after binding, V (L) is the volume of the UA solution, and m (g) is the mass of the polymer used. In the applications with SPR sensors, the concentration and mass parameters are modified. Because there is not a significant change in the concentration of the solution after binding, it is also not possible to exactly determine the mass of the polymer [45]. There is a linear relationship between ΔR% and concentration. For this reason, the selectivity coefficient k is expressed as follows.

$$k = \Delta R_{template}/\Delta R_{competitor} \quad (7)$$

The relative selectivity coefficient, k′ can be expressed:

$$K' = k_{MIP}/k_{NIP} \quad (8)$$

The UA-imprinted SPR sensor was used to analyse a human urine sample. The urine sample was centrifuged at 5000*g* for 15 min at room temperature. The standard addition method was used to prepare a calibration graph for the UA-imprinted SPR sensor responses. Firstly, to prepare a blank solution, the urine sample was diluted in the ratio of 1:20. After that, the samples spiked with 5, 10, 15, 20, 25, 30 mg/L UA solutions in the same dilution ratio were prepared at pH 8.0. An enzymatic method (COBAS INTEGRA Uric Acid ver. 2 (UA2), Rotkreuz, Switzerland) was also used to determine the UA concentration in the human urine sample. The results were compared with that of the SPR sensor.

3. Results and discussion

3.1. Preparation of the MAC-Fe^{3+}-UA pre-polymerization complex

3.1.1. Characterization of the functional monomer

The functional monomer, MAC, was synthesized as the metal-complexing ligand and characterized using FTIR and NMR spectroscopy. The FTIR and NMR spectra of the MAC monomer and a detailed discussion about the chemical structure are given in Fig. SI2 a and b, respectively.

3.1.2. Potentiometric titrations and preparation of the pre-polymerization complex (MAC-Fe^{3+}-UA)

Non-covalent imprinting is the most commonly used approach in the preparation of molecularly imprinted polymers, because the preorganization step and the removal of the template molecule are simply carried out. It is also possible to find functional monomers that can interact with almost any kind of template molecule. However, the binding affinity of MIPs prepared by non-covalent imprinting is lower than the affinity of MIPs prepared by covalent imprinting. When compared to the template molecule, an excess amount of the functional monomer is used in order to obtain the required amount of template-monomer complex in non-covalent imprinting. In practice, there is an equilibrium between the template molecule and the functional monomer, and it is necessary to add an excess amount of the functional monomer to shift the equilibrium towards the formation of the template-monomer complex. As a result, template-monomer complexes form in different configurations, and heterogeneous binding sites with different affinity constants are obtained in the prepared final MIP [46].

In the metal-ion-mediated imprinting approach, a coordination bond between a template molecule and a functional molecule is constituted via metal ions. Coordinate bonds are more specific than non-covalent interactions. In addition, it is possible to form or cleave coordinate bonds by changing the external pH. Thus, metal-ion-mediated imprinting is an important alternative to traditional imprinting methods [47].

In this study, MAC, a cysteine derivative, was preferred as a functional monomer and used as a metal-complexing ligand in the preorganization step. Parr and Pearson classify a thiolate group as a soft base [48,49]. Therefore, the affinity of the thiolate group (SH) to the soft metal ions, e.g., Hg^{2+} and Pd^{2+} is high. However, it is possible to obtain stable mixed ligand complexes in the presence of molecules containing harder groups (e.g., COOH and NH_2) with hard metal ions (e.g., Mn^{2+} and Fe^{3+}) [50]. Uric acid is a diprotic acid with two ionisable protons, as shown in Fig. SI3. Metal–urate complexes with different metals—such as Ni, Cr, Co, Mn, Cd, Fe, Na, Cu, K and UO_2—were synthesized and characterized [51].

To prepare UA-imprinted nanoparticles, a metal-ion-mediated strategy was used in the preorganization step. A sulfhydryl group (—SH) containing MAC was selected as a functional monomer and/or metal chelating ligand for the interaction with UA (template molecule) via Fe^{3+} ion-mediated coordination. It is known that UA molecule forms stable complexes with Fe^{3+} ions [51].

By taking the advantage of possible MAC-Fe^{3+} and UA-Fe^{3+} interactions, formation of MAC-Fe^{3+}-UA mixed ligand complex was investigated using the potentiometric titration method. The main objective was to obtain valuable parameters for UA/Fe^{3+}/MAC mol ratio and bond formation/cleavage conditions in the mixed ligand complex, which could be used to achieve high selectivity and affinity towards UA molecule in the UA-imprinted nanoparticles.

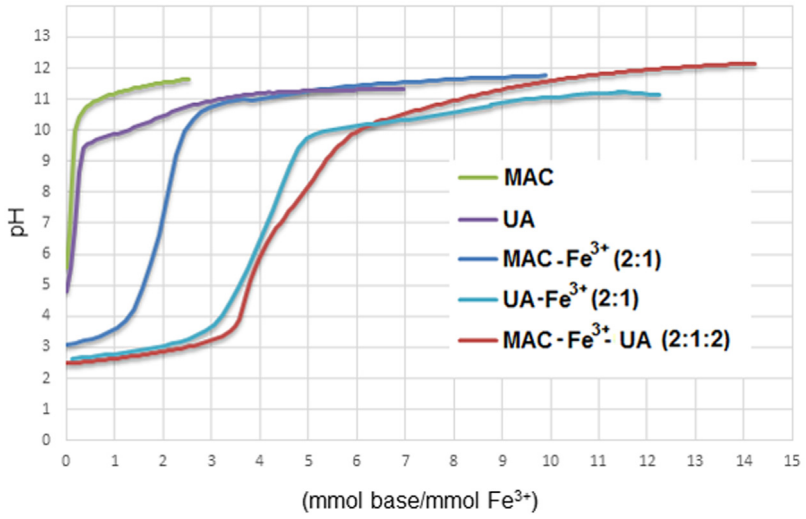


Fig. 1. Titration curves for MAC, UA, MAC-Fe^{3+}, UA-Fe^{3+} and MAC-Fe^{3+}-UA systems.

MAC, UA aqueous solutions and MAC-Fe^{3+}, UA-Fe^{3+} and MAC-Fe^{3+}-UA mixtures prepared in various metal-to-ligand ratios were titrated with 0.01 M KOH solution using the potentiometric titration method at 25 °C. All the titration curves that plotted mmol base/mmol Fe^{3+} (m) versus pH are depicted in Fig. 1. In comparison with MAC and UA titration curves, the shifts in the inflection points of MAC-Fe^{3+}, UA-Fe^{3+} and MAC-Fe^{3+}-UA titration curves demonstrate the complex formation in the studied mixtures. In the MAC-Fe^{3+} complex (2:1 mol ratio) titration curve, the m value is 2. This means that MAC has one ionizable –SH group and binds to Fe^{3+} ion in the complex. Similarly, the m value is 4 for the UA-Fe^{3+} (2:1 mol ratio) titration curve, which shows that there are two ionizable protons. The UA molecule acts as a bidentate ligand in the UA-Fe^{3+} complex. According to data obtained from the MAC-Fe^{3+} and UA-Fe^{3+} titration curves, the MAC-Fe^{3+}-UA mixture in the mol ratio of 2:1:2 was titrated with 0.01 M KOH solution at 25 °C. There are two inflection points in the titration curve of MAC-Fe^{3+}-UA mixed ligand complex (2:1:2) at pH 3.5 and pH 7.0. At pH 3.5, the MAC-Fe^{3+} complex forms and then at pH 7.0, the MAC-Fe^{3+}-UA mixed ligand complex in the mol ratio of 2:1:2 forms via UA binding to MAC-Fe^{3+} complex. As a result, the six coordination sites of the Fe^{3+} ion are filled with two MAC monodentate ligands and two UA bidentate ligands. The proposed structure for the MAC-Fe^{3+}-UA pre-polymerization complex is given in Fig. SI4.

3.1.3. FTIR analysis

In order to show MAC-Fe^{3+}complex and MAC-Fe^{3+}-UA mixed ligand complex formation, the complexes were prepared using the data obtained from potentiometric titration. Then, the complexes were characterized using FTIR analyses. Fig. SI5 depicts the FTIR spectra of the MAC and MAC-Fe^{3+} complex. The results of the analyses were discussed in the supplementary information.

3.2. Characterization of poly(HEMA-MAC)-Fe^{3+}nanoparticles

The imprinting of template molecules into nanoparticles provide more homogeneous binding sites. Also, the binding sites are on the surface or inside the nanoparticles. In addition, since the template molecule can be completely removed, the number of specific binding sites is greater. Thus, it is possible to obtain higher adsorption rates and capacities. To prepare the nanoparticles highly selective for uric acid, MAC–Fe^{3+}-UA pre-polymerization complex (prepared according to the UA: Fe^{3+}:MAC mol ratio [2:1:2]) was copolymerized with HEMA by emulsion polymerization in the presence of cross-linker EGDMA. After the synthesis, the nanoparticles were characterized using FTIR analysis. The FTIR spectrum is depicted in Fig. SI6 and discussed in detail. The proposed chemical structure for the poly(HEMA-MAC)-Fe^{3+} nanoparticle is also shown in Fig. SI7.

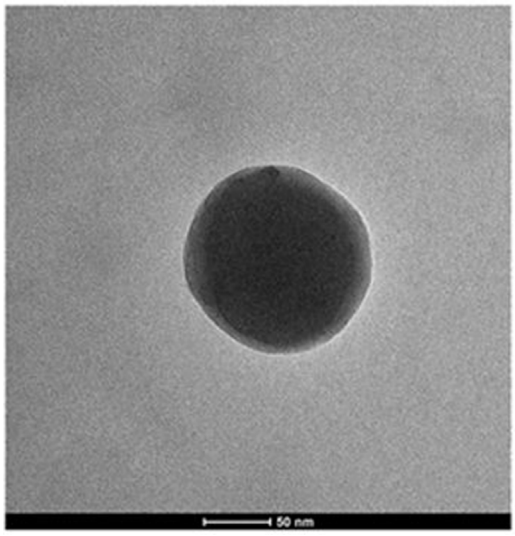


Fig. 2. TEM micrograph of UA-imprinted poly(HEMA-MAC)-Fe^{3+}nanoparticle.

The TEM micrograph of the UA-imprinted poly(HEMA-MAC)-Fe^{3+} nanoparticle is shown in Fig. 2. As it shows, the nanoparticle has a spherical structure and a particle diameter of around 100 nm. The results showed that the polymerization procedure is suitable for preparing the UA-imprinted poly(HEMA-MAC)-Fe^{3+}nanoparticles.

To obtain additional insight into the morphology of UA-imprinted poly(HEMA-MAC)-Fe^{3+} nanoparticles, SEM analysis was also conducted. The UA-imprinted nanoparticles were first dried and then SEM photographs were taken. As can be seen from the SEM photograph in Fig. SI8, the nanoparticles are very small and aggregate after drying. EDS analysis combined with SEM shows that the elemental composition of the sample was conducted. The elemental composition of the poly(HEMA-MAC)-Fe^{3+} nanoparticles is also summarized in Fig. SI9. The existence of Fe atoms in the composition demonstrates that poly(HEMA-MAC)-Fe^{3+} nanoparticles were synthesized successfully.

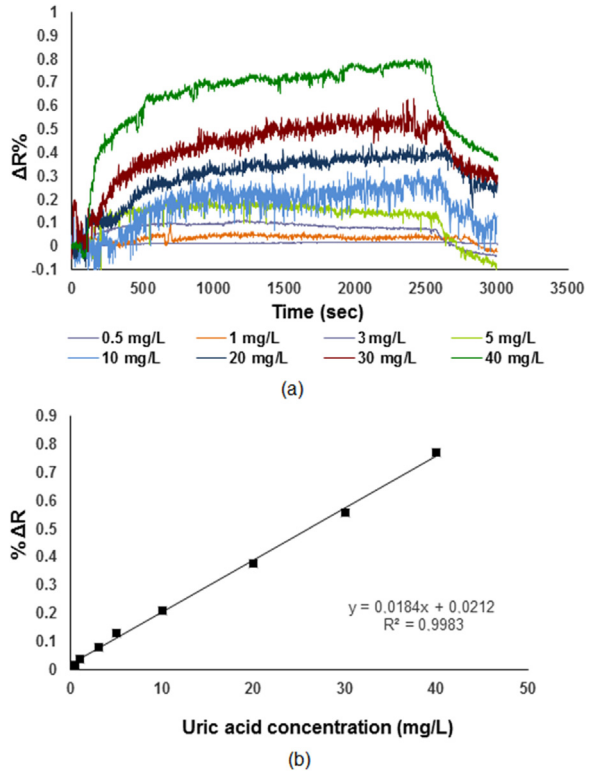


Fig. 3. (a) SPR sensorgrams for aqueous UA solutions in the concentration range of 0.5 mg/L to 40 mg/L and (b) concentration dependency of the UA-imprinted SPR sensor.

Zeta size analysis was used to gain valuable information about the size distribution of the UA-imprinted poly(HEMA-MAC)-Fe^{3+} nanoparticles in aqueous solution. Figure SI10 shows the size distribution graph of UA-imprinted poly(HEMA-MAC)-Fe^{3+}nanoparticles. The average diameter and polydispersity index (PDI) of the nanoparticles were determined as 117.8 nm and 0.223, respectively. The polydispersity index shows aggregation in the nanoparticles. In addition, PDI values in the range of 0.1–0.25 reflect a narrow size distribution, and a PDI value higher than 0.5 indicates a broad distribution [54]. According to the results, UA-imprinted poly(HEMA-MAC)-Fe^{3+} nanoparticles have a narrow size distribution and can be used for sensor preparation.

3.3. Characterization of UA-imprinted SPR sensor surface

The-UA imprinted poly(HEMA-MAC)-Fe^{3+} nanoparticles were integrated into the SPR gold surface for sensor preparation. In order to characterize the UA-imprinted SPR sensor, contact angle measurements, AFM analysis and optical profilometer analysis were conducted. The detailed discussions of the characterization are included in the supporting information. According to the results, the UA-imprinted sensor was successfully performed.

3.4. Kinetic studies with UA-imprinted SPR sensor

Firstly, UA-imprinted poly(HEMA-MAC)-Fe^{3+}SPR was interacted with aqueous UA solutions. And, SPR sensorgrams were prepared for UA solutions in concentrations ranging from 0.5 mg/L to 40 mg/L (Fig. 3a). The aqueous UA solutions caused an increase in the SPR sensor response and a plateau was achieved in about 15 min. A solution at pH 8.0 was used to remove non-specifically bound UA molecules from the SPR sensor surface. The minimum UA concentration that causes a sensor response was 0.5 mg/L. The sensor response increased linearly until a UA concentration of 40 mg/L. Because of the low solubility of UA in aqueous solution (pH 8.0) [56], the higher UA concentration could not be studied with the prepared SPR sensor.

Fig. 3b shows the linear range of the UA-imprinted SPR sensor. The calibration graph depicts that correlation is high (R^2 = 0.9983). The limit of detection (LOD) and limit of quantitation (LOQ) values of the UA imprinted SPR sensor were calculated from the data obtained in the concentration range of 0.5 mg/L to 40 mg/L. The standard deviation of sensor response obtained for the minimum UA concentration (0.5 mg/L) was used for the calculation. LOD and LOQ values were determined as 0.247 mg/L and 0.825 mg/L, respectively. LOD values of the sensors using imprinted polymers as the molecular recognition element to detect UA are summarized in Table 1.

3.5. Kinetic and isotherm analysis of UA-imprinted SPR sensor data

The SPR sensor responses obtained from kinetic analyses of aqueous UA solutions were used to determine kinetic and isothermal parameters. The kinetic parameters were calculated by evaluating the fitness of SPR data to the equilibrium kinetic analysis model. Langmuir, Freundlich and Langmuir-Freundlich (Sips) isotherm models were used for isothermal analyses. The Freundlich isotherm model shows the multilayer binding of analyte molecules, while the Langmuir isotherm model relies on the assumption that the binding sites are homogeneous. The Langmuir-Freundlich model is derived from the limiting behaviour of the Langmuir and Freundlich isotherm models [57]. The Langmuir-Freundlih model is reduced to the Freundlich isotherm model at low analyte concentrations and to the Langmuir isotherm model at high analyte concentrations.

The parameters of the kinetic and isothermal analyses are shown in Table 2. When we examine the correlation coefficients, it can be clearly seen that the data fit well with the Langmuir (R^2 = 0.996), Freundlich (R^2 = 0.9975) and Langmuir-Freundlich (R^2 = 0.9953) isotherm models. However, the calculated ΔR_{maks} value according to Langmuir isotherm model is close to the experimental ΔR_{maks} value. The Freundlich isotherm equation assumes that binding sites are heterogeneous and that each binding-site class obeys the Langmuir equation. In addition, the amount of adsorption increases infinitely with increasing concentrations. Thus, the Freundlich equation is more meaningful at low concentrations. The SRP sensor data were only obtained in the concentration range of 0.5 mg/L to 40 mg/L due to the low solubility of UA (40 mg/L). Therefore, the Freundlich isotherm model is as fitted as the Langmuir isotherm model with high correlation coefficients.

3.6. Selectivity of the UA-imprinted SPR sensor

In order to show the selectivity of the UA-imprinted SPR sensor, UA, ascorbic acid (AA), theophylline (Teo) and urea (U) were used as competitor molecules. Urea and ascorbic acid were selected due to the existence in real biological samples. Theophylline was selected for similarity in chemical structure to UA. Chemical structure and acid/base ionization constants of the competing molecules are shown in Table SI2.

The solutions of competing biomolecules were prepared and sensorgrams for interaction were recorded using the SPRImager II system. The sensor responses (ΔR%) of the UA-imprinted SPR sensor for UA, AA, Teo and U are shown in Fig. 4a. As shown, the ΔR% values for AA, Teo and U were lower than that for UA due to the high selectivity of the UA-imprinted SPR sensor. Fig. 4b shows the sensor responses (ΔR%) of the non-imprinted SPR sensor. The results show that the non-imprinted SPR sensor does not give a significant signal response for UA, AA, Teo and U. The selectivity coefficients for

Table 1
LOD values of the sensors using imprinted polymers as a recognition element.

Imprinted polymer	Method	LOD	Reference
Amine–imide type conducting polymer	Amperometric	0.05 mg/L	[33]
Silica gel-bonded molecularly imprinted polymer	Voltametric	0.024 mg/L	[29]
Polymethacrylic acid coated MWCNTs	Amperometric	3.7 mg/L	[39]
Acrylic acid	Stripping voltammetry	0.0168 mg/L	[35]
Poly(HEMA-MAC)-Fe^{3+} nanoparticles	SPR	0.247 mg/L	This study

Table 2
Parameters of Langmuir, Freundlich and Langmuir-Freundlich isotherm models and kinetic analysis.

Langmuir		Freundlich		Langmuir-Freundlich	
ΔR_{maks},mg/L	0.547	ΔR_{maks}, mg/L	29,04	ΔR_{maks}, mg/L	1.715
K_D, L/mg	13.88	$1/n$	0,8189	$1/n$	0.8189
K_A, mg/L	0.072	R^2	0,9975	K_D, L/mg	44.97
R^2	0.9960			K_A, mg/L	0.022
				R^2	0.9953
Equilubrium kinetic analysis					
k_a, *mg/L s*	1.27×10^{-2}				
k_d, 1/s	1.69×10^{-2}				
R^2	0.9653				

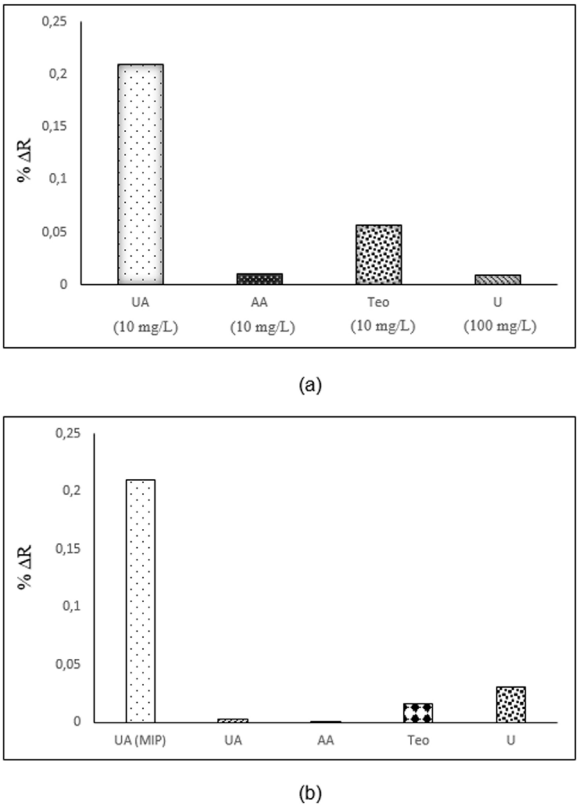


Fig. 4. (a) UA-imprinted sensor responses for UA, AA, Teo and U (b) non-imprinted SPR sensor responses for UA, AA, Teo and U.

the UA-imprinted (MIP) and the non-imprinted (NIP) SPR sensors and the relative selectivity coefficients are shown in Table 3. The results presented in Table 3 demonstrate that specific binding sites for UA were successfully constituted using a metal-ion imprinting approach. The non-imprinted SRP sensor may have suitable functional groups for the binding process, but there are no selective binding cavities. The selectivity coefficients for AA, Teo and U were determined to be 21.0, 3.68 and 23.33, respectively. The relative selectivity coefficients of UA-imprinted SPR sensor for UA/AA, UA/Teo, and UA/U were 6.28, 20.44 and 243.02, respectively. The SPR sensorgrams and graphs show that the UA-imprinted and non-imprinted SPR sensor responses for binary, triple and quadruple mixtures of the competitor molecules are also shown in Fig. SI14.

Table 3
The selectivity and relative selectivity coefficients for competing biomolecules.

Biomolecule	MIP		NIP		
	ΔR	k	ΔR	k	k'
Uric Acid	0.210	–	0.003	–	
Ascorbic Acid	0.010	21.0	0.001	3	6.288
Theophylline	0.057	3.68	0.016	0.18	20.44
Urea	0.009	23.33	0.031	0.096	243.02

The molecular imprinting method utilizing metal coordination interactions is attractive for obtaining highly specific and stable recognition sites for separation of biomolecules, including like proteins [58]. In order to form highly specific recognition sites complementary to the template, the stoichiometric amount of the metal ion needed to bridge the specific interaction between the template and the monomer with high stability is necessary due to structural and spatial complementary to template [59]. In this study, the functional monomer, MAC, assembles around the Fe^{3+} ions and enables preparation of the specific binding site for UA after polymerization. The relative selectivity shows that the binding sites constituted in the imprinted poly(HEMA-MAC)-Fe^{3+} nanoparticles recognize UA preferentially (Fig. 5).

3.7. Urine analysis with UA-imprinted SPR sensor

A UA-imprinted SPR sensor was used to determine UA in urine. The analysis was conducted by using a urine sample taken from a healthy person. The SPR sensorgrams were obtained for urine samples spiked with 5, 10, 15, 20, 25 and 30 mg/L (in pH 8.0) UA in the dilution ratio of 1:20 and for a blank solution in the same dilution ratio. Fig. 6a and b clearly shows that the SPR sensor response increases with the increase in the concentration of UA in the urine samples. The remarkable sensor response for the blank solution results from the non-specific interaction of other molecules in urine. However, the spiked urine samples are in the same dilution ratio and the increase in sensor response is due to the increase in UA concentration. The imprinted SPR sensor shows linearity in a range of 5 mg/L to 20 mg/L. LOD and LOQ values for the urine sample were determined as 0.498 mg/L and 1.66 mg/L, respectively. The UA concentration in the non-diluted urine of as determined as 40.9 mg/L. The UA concentration in the non-diluted

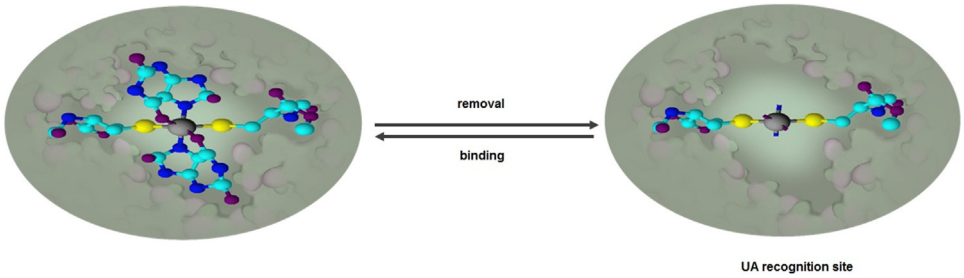


Fig. 5. Recognition mechanism in the binding sites of UA-imprinted poly(HEMA-MAC)-Fe^{3+} nanoparticles.

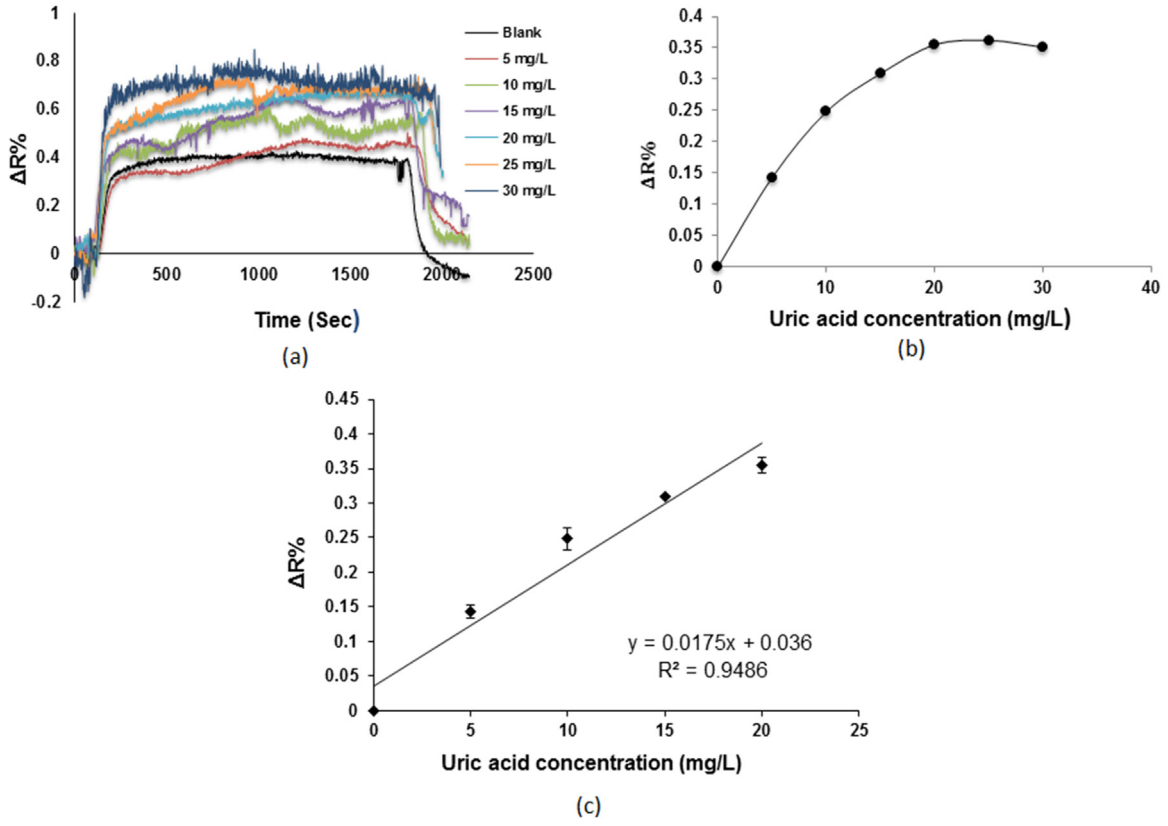


Fig. 6. (a) SPR sensorgrams for urine samples (1:20 dilution), concentration dependency of the SPR sensor (b) in the range of 0.5 mg/L to 30 mg/L and (c) in the range of 0.5 mg/L to 20 mg/L.

urine sample was also determined using the enzymatic method (COBAS INTEGRA Uric Acid ver.2 (UA2), Rotkreuz, Switzerland). The UA concentration was 40 mg/L. It is clear that the UA-imprinted SPR sensor can determine the concentration of UA in urine with high accuracy when compared to the enzymatic method.

There is average 250–750 mg (1.48–4.43 mmol) UA in a 24-h urine sample from a healthy person [64]. In case of diseases such as Lesch-Nyhan syndrome, hyperuricemia and hypertension, the UA level decreases or increases. The normal levels of UA for a healthy person are 130–670 mg/L and 370–920 mg/L for 24-h urine and morning urine, respectively [65]. LOD (0.498 mg/L) and LOQ (1.66 mg/L) values obtained for the UA-imprinted SPR sensor in urine enable the detection of UA. LOD values of some analysis methods for UA in urine are shown in Table 4.

Table 4
LOD values of some analysis methods for UA in urine.

Method	LOD (mg/L)	References
Voltammetric biosensor	0.168	[60]
RP-HPLC	0.210	[61]
Microchip capillary electrophoresis with electrochemical detection	0.168	[5]
Enzymatic biosensor	0.017	[62]
HPLC method	0.110	[63]
MIP SPR sensor	0.498	This study

3.8. Reusability

The reusability of the imprinted SPR sensor was investigated by repeating five equilibration-adsorption-regeneration cycles. A urine sample (1:20 diluted) spiked with 35 mg/L UA was used to obtain the SPR sensorgrams. The SPR sensorgrams for the five consecutive cycles are shown in Fig. SI16. The results demonstrate that the imprinted SPR sensor can be used repeatedly. In addition, the SPR sensor responses are reproducible. The average of the sensor responses (ΔR%) obtained for five consecutive measurements is 0.362 with a standard deviation of 0.0143. Relative standard devi-

ation (RSD) is 3.95%. The small RSD value also demonstrates the repeatability of the measurements.

4. Conclusion

In this study, a metal-ion-mediated strategy of molecular imprinting was used to prepare nanoparticles for specific binding of UA. The preorganization step was investigated using potentiometric titration and the mol ratio of the pre-polymerization complex was determined as 2:1:2 for the functional monomer (MAC):Fe^{3+}:template molecule (UA). Emulsion polymerization was used for the synthesis of UA-imprinted poly(HEMA-MAC)-Fe^{3+} nanoparticles. The UA-imprinted nanoparticles were used as a recognition element in the SPR gold surface. The UA-imprinted SPR sensor was successfully used to detect UA in both aqueous solutions and urine samples. The response time of the SPR sensor is 15 min. LOD and LOQ values for urine samples were determined as 0.498 mg/L and 1.66 mg/L, respectively. The LOD and LOQ values in urine are suitable for UA detection in case of diseases. The isothermal and kinetic parameters for UA binding to the SPR sensor were also investigated. The prepared sensor has high selectivity to UA and also can be used repeatedly with reproducible results.

Acknowledgement

This work was supported by the Research Foundation of Uludag University (Project No: OUAP-2016/4).

Appendix A. Supplementary data

Supplementary data associated with this article can be found, in the online version, at http://dx.doi.org/10.1016/j.snb.2017.05.079.

References

[1] F. Perticone, R. Maio, J.E. Tassone, M. Perticone, A. Pascale, A. Sciacqua, G. Sesti, Interaction between uric acid and endothelial dysfunction predicts new onset of diabetes in hypertensive patients, Int. J. Cardiol. 167 (1) (2013) 232–236.
[2] K. Inoue, T. Namiki, Y. Iwasaki, Y. Yoshimura, H. Nakazawa, Determination of uric acid in human saliva by high-performance liquid chromatography with amperometric electrochemical detection, J. Chromatogr. B 785 (2003) 57–63.
[3] V.L. Star, M.C. Hochberg, Prevention and management of gout, Drugs 45 (1993) 212–222.
[4] R.C. Matos, M.A. Augelli, C.L. Lago, L. Angnes, Flow injection analysis-amperometric determination of ascorbic and uric acids in urine using arrays of gold microelectrodes modified by electrodeposition of palladium, Anal. Chim. Acta 404 (2000) 151–157.
[5] J.C. Fanguy, C.S. Henry, The analysis of uric acid in urine using microchip capillary electrophoresis with electrochemical detection, Electrophoresis 23 (2002) 767–773.
[6] R.D. Monk, Clinical approach to adults, Semin. Nephrol. 16 (1996) 375–388.
[7] Y. Zuo, Y. Yang, Z. Zhu, W. He, Z. Aydin, Determination of uric acid and creatinine in human urine using hydrophilic interaction chromatography, Talanta 83 (2011) 1707–1710.
[8] A. Ascherio, P.A. LeWitt, K. Xu, S. Elberly, A. Watts, W.R. Matson, C. Marras, K. Kieburtz, A. Rudolph, M.B. Bogdanov, S.R. Schwid, M. Tennis, C.M. Tanner, M.F. Beal, A.E. Lang, D. Oakes, S. Fahn, I. Shoulson, M.A. Schwarzchild, Parkinson Study Group DATATOP Investigators, urate as a predictor of the rate of clinical decline in Parkinson disease, Arch. Neurol. 66 (2009) 1460–1468.
[9] T.V. Feichtmeier, H.T. Wrenn, Direct determination of uric acid using uricase, Am. J. Clin. Pathol. 25 (1955) 833–839.
[10] I.D.P. Wootton, H. Freeman, Microanalysis in Medical Biochemistry, 6th ed., Churchill Livingstone, New York, 1982.
[11] D.L. Rocha, F.R.P. Rocha, A flow-based procedure with solenoid micro-pumps for the spectrophotometric determination of uric acid in urine, Microchem. J. 94 (2010) 53–59.
[12] K.M. Kim, G.N. Henderson, X. Ouyang, R.F. Frye, Y.Y. Sautin, D.I. Feig, R.J. Johnson, A sensitive and specific liquid chromatography–tandem mass spectrometry method for the determination of intracellular and extracellular uric acid, J. Chromatogr. B 877 (2009) 2032–2038.
[13] J. Perello, P. Sanchis, F. Grases, Determination of uric acid in urine, saliva and calcium oxalate renal calculi by high-performance liquid chromatography/mass spectrometry, J. Chromatogr. B 824 (2005) 175–180.
[14] S. Piermarini, D. Migliorelli, G. Volpe, R. Massoud, A. Pierantozzi, C. Cortese, G. Palleschi, Uricase biosensor based on a screen-printed electrode modified with Prussian blue for detection of uric acid in human blood serum, Sens. Actuators B: Chem. 179 (2013) 170–174.
[15] S.M.U. Ali, N.H. Alvi, Z. Ibupoto, O. Nur, M. Willander, B. Danielsson, Selective potentiometric determination of uric acid with uricase immobilized on ZnO nanowires, Sens. Actuators B: Chem. 152 (2011) 241–247.
[16] D. Yao, A.G. Vlessidis, N.P. Evmiridis, Microdialysis sampling and monitoring of uric acid in vivo by a chemiluminescence reaction and an enzyme on immobilized chitosan support membrane, Anal. Chim. Acta 478 (2003) 23–30.
[17] M.R. Wightman, L.J. May, A.C. Michael, Detection of dopamine dynamics in the brain, Anal. Chem. 60 (1988) 769–779.
[18] J.M. Zen, J.J. Jou, G. Ilangovan, Selective voltammetric method for uric acid detection using pre-anodized nafion-coated glassy carbon electrodes, Analyst 123 (1998) 1345–1350.
[19] J. Wang, T. Golden, T. Peng, Poly(4-vinylpyridine)-coated glassy carbon flow detectors, Anal. Chem. 59 (1987) 740–744.
[20] L.D. Spurlock, A. Jaramillo, A. Praserthdam, L.J. Lewis, A. Brajter-Toth, Selectivity and sensitivity of ultrathin purine-templated overoxidized polypyrrole film electrodes, Anal. Chim. Acta 336 (1–3) (1996) 37–46.
[21] P.R. Roy, T. Okajima, T. Ohsaka, Simultaneous electrochemical detection of uric acid and ascorbic acid at a poly(*N*,*N*-dimethylaniline) film-coated GC electrode, J. Electroanal. Chem. 561 (2004) 75–82.
[22] A.M. Yu, H.L. Zhang, H.Y. Chen, Catalytic oxidation of uric acid at the polyglycine chemically modified electrode and its trace determination, Analyst 122 (1997) 839–841.
[23] J.A. Ni, H.X. Ju, H.Y. Chen, D. Leech, Amperometric determination of epinephrine with an osmium complex and nafion double-layer membrane modified electrode, Anal. Chim. Acta 378 (1999) 151–157.
[24] J.M. Zen, C.T. Hsu, A selective voltammetric method for uric acid detection at nafion(*R*)-coated carbon paste electrodes, Talanta 46 (1998) 1363–1369.
[25] S.B. Khoo, F. Chen, Studies of sol-gel ceramic film incorporating methylene blue on glassy carbon: an electrocatalytic system for the simultaneous determination of ascorbic and uric acids, Anal. Chem. 74 (2002) 5734–5741.
[26] C.R. Raj, T. Ohsaka, Voltammetric detection of uric acid in the presence of ascorbic acid at a gold electrode modified with a self-assembled monolayer of heteroaromatic thiol, J. Electroanal. Chem. 540 (2003) 69–77.
[27] X. Cai, K. Kalcher, C. Neuhold, B. Ogorevc, An improved voltammetric method for the determination of trace amounts of uric acid with electrochemically pretreated carbon paste electrodes, Talanta 41 (1994) 407.
[28] J.M. Zen, P.J. Chen, A selective voltammetric method for uric acid and dopamine detection using clay-modified electrodes, Anal. Chem. 69 (1997) 5087–5093.
[29] B.B. Prasad, P.S. Sharma, D. Lakshmi, Molecularly imprinted polymer-based solid-phase extraction combined with molecularly imprinted polymer-based sensor for detection of uric acid, J. Chromatogr. A 1173 (2007) 18–26.
[30] S. Chuekachang, R. Janmanaee, A. Baba, S. Phanichphant, S. Sriwichai, K. Shinbo, K. Kato, F. Kaneko, N. Fukunda, H. Ushijma, Fabrication of thin film fromconducting polymer/single wall carbon nanotube composites for the detection of uric acid, Mol. Cryst. Liq. Cryst. 1 (2013) 1–6.
[31] K.Z. Kamali, A. Pandikumar, G. Sivaraman, H.N. Lim, S.P. Wren, T. Sun, N.M. Huang, Silver@graphene oxide nanocomposite-based optical sensor platform for biomolecules, RSC Adv. 5 (23) (2015) 17809–17816.
[32] N. Misraa, V. Kumar, L. Borde, L. Varshneya, Localized surface plasmon resonance-optical sensors based on radiolytically synthesized silver nanoparticles for estimation of uric acid, Sens. Actuators B: Chem. 178 (2013) 371–378.
[33] P. Chena, R. Vittal, P. Niena, G. Lioub, K. Hoa, A novel molecularly imprinted polymer thin film as biosensor for uric acid, Talanta 80 (2010) 1145–1151.
[34] C. Zhang, S. Si, Z. Yang, A highly selective photoelectrochemical biosensor for uric acid based on core-shell Fe3O4@C nanoparticle and molecularly imprinted TiO_2, Biosens. Bioelectron. 65 (2015) 115–120.
[35] R.V. Motghare, K.K. Tadi, P. Dhawale, S. Deotare, A.K. Kawadkar, R. Chillawar, S. Khan, Voltammetric determination of uric acid based on molecularly imprinted polymer modified carbon paste electrode, Electroanalysis 27 (3) (2015) 825–832.
[36] A. Mujahid, A. Khan, A. Afzal, T. Hussain, M.H. Raza, A.T. Shah, W. Zaman, Molecularly imprinted titania nanoparticles for selective recognition and assay of uric acid, Appl. Nanosci. 5 (5) (2015) 527–534.
[37] H.T. Lian, Z.H. Sun, X.Y. Sun, B. Liu, Graphene doped molecularly imprinted electrochemical sensor for uric acid, Anal. Lett. 45 (18) (2012) 2717–2727.
[38] J.F. Yin, H.T. Lian, X.Y. Sun, B. Liu, Highly selective determination of uric acid in human serum by molecularly imprinted electrochemical sensor, J. Huaqiao Univ. (Nat. Sci.) 33 (1) (2012) 33–38.
[39] P.Y. Chen, P.C. Nien, C.W. Hu, K.C. Ho, Detection of uric acid based on multi-walled carbon nanotubes polymerized with a layer of molecularly imprinted PMAA, Sens. Actuators B: Chem. 146 (2) (2010) 466–471.
[40] A.K. Patel, P.S. Sharma, B.B. Prasad, Electrochemical sensor for uric acid based on a molecularly imprinted polymer brush grafted to tetraethoxysilane derived sol-gel thin film graphite electrode, Mater. Sci. Eng. C 29 (5) (2009) 1545–1553.
[41] D. Lakshmi, P.S. Sharma, B.B. Prasad, Development of uric acid sensor based on molecularly imprinted polymer-modified hanging mercury drop electrode, Electroanalysis 18 (9) (2006) 918–927.
[42] G. Schwarzenbach, H. Flaschka, Complexometric Titrations, Interscience Publishers, New York, 1969.

[43] M. Sarı, S. Akgol, M. Karataş, A. Denizli, Reversible immobilization of catalase by metal chelate affinity interaction on magnetic beads, Ind. Eng. Chem. Res. 45 (2006) 3036–3043.
[44] B. Osman, L. Uzun, N. Besirli, A. Denizli, Microcontact imprinted surface plasmon resonance sensor for myoglobin detection, Mater. Sci. Eng. C 33 (2013) 3609–3614.
[45] L.P. Lin, L.S. Huang, C.W. Lin, C.K. Lee, J.L. Chen, S.M. Hsu, S. Lin, Determination of binding constant of DNA-binding drug to target DNA by surface plasmon resonance biosensor technology, Curr. Drug Target 5 (2005) 61–72.
[46] C.C. Hwang, W.C. Lee, Chromatographic characteristic of cholesterol-imprinted polymers prepared by covalent and non-covalent imprinting methods, J. Chromatogr. A 962 (2002) 69–78.
[47] K. Çetin, A. Denizli, 5-Fluorouracil delivery from metal-ion mediated molecularly imprinted cryogel discs, Colloids Surf. B 126 (2015) 401–406.
[48] R.G. Pearson, Hard and soft acids and bases, J. Am. Chem. Soc. 85 (1963) 3533–3539.
[49] R.G. Parr, R.G. Pearson, Absolute hardness: companion parameter to absolute electronegativity, J. Am. Chem. Soc. 105 (1983) 7512–7516.
[50] H. Pesonen, R. Aksela, K. Laasonen, Density functional complexation study of metal ions with cysteine, J. Phys. Chem. A 114 (2010) 466–473.
[51] M.S. Masoud, A.E. Ali, M.A. Shaker, G.S. Elasala, Synthesis, computational, spectroscopic, thermal and antimicrobial activity studies on some metal-urate complexes, Spectrochim. Acta Part A: Mol. Biomol. Spectrosc. 90 (2012) 93–108.
[54] L. Wu, J. Zhang, W. Watanabe, Physical and chemical stability of drug nanoparticles, Adv. Drug Deliv. Rev. 63 (2011) 456–469.
[56] W.N. Kelley, I.M. Weiner, Uric Acid, Springer-Verlag, Berlin, Heidelberg, New York, 1978 (Chapter 14).
[57] K.Y. Foo, B.H. Hameed, Insights into the modeling of adsorption isotherm systems, Chem. Eng. J. 156 (1) (2010) 2–10.
[58] E. Tamahkar, A. Denizli, Metal ion coordination interactions for biomolecule recognition: a review, Hittite J. Sci. Eng. 1 (1) (2014) 21–26.
[59] S. Chaitidou, O. Kotrotsiou, C. Kiparissides, On the synthesis and rebinding properties of [$Co(C_2H_3O_2)_2$(z-histidine)] imprinted polymers prepared by precipitation polymerization, Mater. Sci. Eng. C 29 (2009) 1415–1421.
[60] E.M. Strochkova, Y.I. Turyan, I. Kulseman, A. Shenhar, Simultaneous voltammetric determination of uric and ascorbic acids in urine, Talanta 44 (1997) 1923.
[61] Y. Yue-dong, Simultaneous determination of creatine uric acid, creatinine and hippuric acid in urine by high performance liquid chromatography, Biomed. Chromatogr. 12 (1998) 47–49.
[62] E. Akyılmaz, M.K. Sezgintürk, E. Dinçkaya, A biosensor based on urate oxidase-peroxidase coupled enzyme system for uric acid determination in urine, Talanta 61 (2) (2003) 73–79.
[63] S.K. George, M.T. Dipu, U.R. Mehra, P. Singh, A.K. Verma, J.S. Ramgaokar, Improved HPLC method for the simultaneous determination of allantoin, uric acid and creatinine in cattle urine, J. Chromatogr. B 832 (1) (2006) 134–137.
[64] N.W. Tietz, Clinical Guide to Laboratory Tests, 3rd ed., W.B. Saunders, Philadelphia, 1995.
[65] M. Krieg, K.J. Gunsser, E. Steinhagen-Thiessen, H. Becker, Comparative quantitative clinico-chemical analysis of the characteristics of 24-h urine and morning urine, J. Clin. Chem. Clin. Biochem. 24 (1986) 863–869.

Biographies

Aslı Göçenoğlu Sarıkaya received her BS degree in chemistry from Ege University (2008). She received her MSc. degree (2009) and Ph.D. degree (2015) in Ege University and Uludağ University, respectively. Her research interests are molecularly imprinted polymeric biomaterials, micro/nano materials and their applications.

Bilgen Osman received her Ph.D. degree from Uludağ University in 2011. She is an associate professor at the same university. Her main research areas are enzyme immobilization, synthesis of polymeric materials for removal of toxic compounds, biosensors based on synthetic receptors and molecular imprinting.

Tülay Çam received her Ph.D. degree in 2012. Her main research areas are metal-chelate chemistry and potentiometry.

Adil Denizli is a professor at Hacettepe University, Ankara, Turkey. He received Ph.D. degree from the same university in 1992. His main research fields are molecular imprinting technologies, hemoperfusion-removal of toxic materials from blood, purification of enzymes and proteins by chromatographic methods, biosensors based on synthetic receptor technology, production of polymers have different surface and bulk properties, shape and geometries, application of these polymers in medicine and biology.